FANATIC: AN SIS RADIOMETER FOR RADIO ASTRONOMY IN THE 660–690 GHz BAND

A.I. Harris[1], K.–F. Schuster[1,2], K.–H. Gundlach[2], and B. Plathner[2]

[1]Max Planck Institute for extraterrestrial Physics,
Postfach 1603, D–85740 Garching, Germany
harris@fcrao1.phast.umass.edu

[2]IRAM, 300 rue de la Piscine, Domaine Universitaire de Grenoble,
F-38406 St. Martin d'Heres Cedex, France
schuster@iram.grenet.fr

ABSTRACT

FANATIC is a compact radiometer optimized for radio astronomy from about 660 to 690 GHz ($\lambda\lambda$ 455 – 435 μm). We observed a large number of molecular and atomic spectral lines from galactic and extragalactic sources during *FANATIC* 's first run on the James Clerk Maxwell Telescope in early March 1994. Double sideband receiver temperatures during observations were about 800 K (25 $h\nu/k$). The heart of the receiver is a two-junction Nb/AlO_x/Nb SIS array fed by a sandwiched V-Antenna. The junction array and antenna are fabricated together at IRAM's Grenoble SIS laboratory. Each junction has a normal resistance of $R_n \sim 10\ \Omega$, an area of $\sim 2\ \mu m^2$, an individual radial stub circuit to resonate the capacitance, and a $\lambda/4$ transformer to match to the antenna. The solid-state local oscillator is a mm-wave Gunn oscillator followed by a doubler and tripler. The LO diplexer is a Martin–Puplett interferometer, which insures that there is always abundant LO power for operation and speedy tuning. The receiver and telescope coupling optics, LO, dewar, and calibration system fit on an 0.6 x 0.8 m optical breadboard.

1 INTRODUCTION

Radio astronomy, with its constraints of limited observing time and very weak signals, has benefitted greatly from the decreases in noise temperatures provided by SIS mixers. SIS

(Superconductor-Insulator-Superconductor) tunnel junction mixers have replaced Schottky diode mixers for most radio astronomical applications at millimeter wavelengths, and they are now spreading rapidly on to telescopes at the high end of the submillimeter band [1–5].

We have constructed an SIS mixer receiver, named *FANATIC*, that has now replaced our Schottky diode mixer facility receiver at the James Clerk Maxwell Telescope in Hawaii [6]. *FANATIC* is a compact radiometer optimized for radio astronomy from about 660 to 690 GHz ($\lambda\lambda$ 455 – 435 μm). This frequency range lies within the second-highest atmospheric window at submillimeter wavelengths. This window includes many astrophysically important transitions, including lines from isotopomers of the CO molecule ($C^{18}O$, ^{13}CO, and CO $J = 6-5$) as well as the more density-sensitive CS $J = 14-13$ and $H^{13}CN$ $J = 8-7$ lines.

2 Radiometer Layout

2.1 Mixer and Cryostat

Design considerations for the mixer, its tuning structure, and the fabrication have been recently been described [1,7] so we give only a synopsis here. The mixer is a two-junction SIS tunnel junction array fed by a sandwiched V-Antenna. The junction array and antenna are fabricated together at IRAM's Grenoble SIS laboratory on a 0.4 mm thick piece of fused quartz that is sandwiched between 3 mm thick sub- and superstrates. Eckart et al. [8] found that air gaps within the sandwich bigger than $\lambda/300$ (1.4 μm at 690 GHz) generate surface waves that degrade the antenna performance, so all of the quartz pieces are optically flat and are clamped together without films of glues or oils. Beam profiles show no trace of fine structure that would indicate surface waves. While not the optimum antenna for a current new development, the V-antenna is in fact fairly reasonable (comparable to a smooth-wall conical horn), and it is certainly suitable for a developmental system.

Each of the $Nb/AlO_x/Nb$ junctions in the array has a normal resistance of $R_n \sim 10\ \Omega$, areas of $\sim 2\ \mu m^2$, a short length of transmission line terminated in a radial stub to resonate the capacitance, and a $\lambda/4$ transformer to match to the antenna (Fig. 1). The transformation is made for the optimum power match, as is appropriate at these frequencies [1,7,9].

One of the main concerns in the design was finding structures and parameters were as insensitive as possible to precise relative alignment, taking 1 μm as a reasonable alignment tolerance.

The mixer sandwich is clamped by a solid copper holder attached to a copper block soldered to the vacuum side of the cold plate in an Infrared Laboratories HD-10 dewar. The IF matching network and a superconducting magnet coil also attach to the copper holder. A high permeability Cryoperm structure with a loop in front of the V's mouth and a post behind the mixer concentrates the field along the axis of the "V."

The beam from the V-antenna is fast enough that some reimaging is necessary inside the cryostat to keep the mechanical sizes of optical elements and heat loads at a reasonable level. A single off-axis ellipse reimages the 0.45 mm beamwaist from the V-antenna to a 3.5 mm waist at the cryostat wall (Fig. 2). This ellipse's f/D ratio is small, so keeping the angle of incidence as small as mechanically practical (30°) substantially reduces distortion and cross-polarization losses [10]. The radiation load on the quartz is kept low by reflecting the submillimeter signal from a wire grid and through a hole in a copper shield that surrounds the block. The grid also transmits cross-polarized power from the mixer and elliptical mirror to terminate it inside the cryostat at low temperature. Sensitivity to only one polarization is important because only one polarization is transmitted by the external Martin–Puplett interferometer that combines the LO and signal beams. Drives from outside the cryostat can tilt the grid about two axes to peak up alignment of the internal cryostat optics. A crystalline quartz filter on the liquid nitrogen temperature radiation shield reduces the room temperature heat load on the helium bath. The room-temperature cryostat vacuum window is also crystalline quartz, in this case anti-reflection (AR) coated with TPX $\lambda/4$ foils held in place with a thin layer of silicone glue. The AR coatings have very low loss: the receiver noise temperature was not measurably changed by adding or removing an extra external AR-coated window, and the noise temperature definitely dropped at frequencies away from the uncoated window's resonance. Leak testing did indicate that helium could diffuse into the cryostat from the edge of the vacuum-side TPX layer, but this did not cause any noticeable problems.

Radio-frequency interference pickup is a potential hazard with an open structure mixer, which has poorly shielded input terminals at the front of the entire IF system. The optical entrance into the dewar accordingly includes of a long aluminium tube that is fixed to the outer wall. This tube is sized to yield more than 100 dB attenuation at the high end of the IF band. All electrical leads pass through standard bulkhead RF filters that are soldered to brass houses below each of the hermetic seals on the dewar top plate. The mixer DC bias preamplifier is in a small aluminium box permanently mounted on the dewar, and the control signals to and from the rest of the bias electronics are at volt levels. The dewar case is a very good electrostatic shield, and magnetic pickup is minimized by using a twisted pair of twisted-pair wires for the conventional four-point bias circuit. These precautions solve all pickup problems except occasional flux trapping in one or the other of the junctions when motors switch on near the receiver. Warming the junctions for about 15 seconds with a small heater inside the mixer block solves this problem, however.

The cryogen hold time is adequate for our needs: 16 hours with the first IF amplifier switched on and 36 hours with it switched off.

2.2 Optical and Mechanical

The optical train matches the 3.5 mm beamwaist at the cryostat wall to the 11.8 mm waist necessary to illuminate the telescope properly, provides the diplexer for the LO and signal, and matches the LO horn's 0.77 mm waist to cryostat's beamwaist. Insensitivity to exact beamwaist sizes — a fundamental Gaussian beam analysis is certainly only approximate for the V-antenna — and the small LO beamwaist are the main drivers for magnification in stages. The beam from the dewar is refocussed by a second off-axis elliptical mirror to make a 6 mm beamwaist near the mean center of the diplexer. A third off-axis mirror reimages this intermediate beamwaist to make the 11.8 mm beamwaist required to produce a $\sim$ 13 dB telescope edge taper. The second and third mirrors are separated by approximately the sum of their focal lengths (nearly a Gaussian telescope) as this reduces the sensitivity of the output against small changes in beamwaist sizes, locations, and mirror positions. The 6 mm beamwaist in the diplexer is just big enough to keep the diplexer loss low, but is still reasonable in terms of matching the LO beam. Lowest possible loss in the LO arm

was not a design driver, and a moderate amount of mismatch due to frequency dependence or errors in the large magnification ratio between the horn and intermediate beamwaist is acceptable. The third mirror is pinned in place for accurate relocation. It can be removed easily to let the beam go straight from the diplexer through an ambient chopper wheel and into a liquid nitrogen load for tuning. When the third mirror is in place the beam from the diplexer reflects vertically to the fourth and final mirror, a flat at the height of the telescope's elevation bearing. This flat bends the beam horizontally through a hole in the bearing and has fine adjustments for tilt and height to precisely coalign the receiver's beam with the telescope's optical axis.

The Martin–Puplett interferometer diplexer that combines the LO and sky signals considerably simplifies receiver operation. Tuning is fast because the LO chain need not be tuned to optimum points with several interacting LO adjustments, but just close enough to produce sufficient power. With the high efficiency optics, tuning is limited by the Gunn diode's tuning limits. The main penalty is somewhat decreased optical transmission away from band center, with a power coupling efficiency of

$$\eta = \frac{1}{2}\left[1 + \cos\left(\frac{\Delta\nu}{\nu_{IF}}\pi\right)\right] \tag{1}$$

when the diplexer is set to the minimum distance that couples both sidebands and the LO ($\lambda/4$ one-way path difference). For our ν_{IF} = 1.5 GHz IF center frequency, the maximum loss, at $\Delta\nu = \pm 500$ MHz from band center, is a factor of 1.33 (1.25 dB). In a practical sense we compensate for much of this loss by being able to work more efficiently when the weather is good at the telescope.

Although the V-antenna produces a mostly Gaussian beam, it is only approximately so, and some fraction of the power is in modes that might not couple properly to the calibration loads or telescope. We need to constrain and characterize the beam distributions at the calibration loads, telescope focus, and on the sky to insure that we properly calibrate our astronomical data. One of useful effects of the optics in this respect is that it serves as a kind of spatial filter to clean up the beam from the receiver, diffracting out higher modes that would not couple to the telescope before they reach the calibration system. Counting this spatial filtering effect, we measured the optical train's transmission efficiency by placing a 50% transmission beamsplitter directly in front of the dewar and measuring the total power

with a large cold load; and then by moving the same beamsplitter in front of the calibration load, readjusting the LO attenuator to give the same operating point, and measuring the new power level from the cold load. This method gave a coupling efficiency of 0.8, which includes mode mismatch, power lost to scattering from wide-angle sidelobes, and all other losses.

By the time the beam leaves the receiver, the power is consequently in a well defined Gaussian beam with some power still in a larger scale beam. We decomposed the beam power distribution into a few Gaussian components by measuring the peak power change from a family of liquid-nitrogen temperature disks with known diameters. The power coupling efficiency η of a Gaussian beam of power FWHM θ_b centered on a uniform temperature disk source of diameter D is

$$\eta = 1 - e^{-\ln 2\,(D/\theta_b)^2}. \tag{2}$$

At the telescope it is unusual that a range of planets is available, so it is useful instead to vary the coupling by changing the center-to-center distance between the beam and a planet. When the beam and disk are not concentric the coupling efficiency is reduced by a weighting factor $w(s)$, normalized so $w(0) = 1$:

$$w(s) = \frac{2\alpha e^{-\alpha s^2} \int_0^R e^{-\alpha r^2} \mathrm{I}_0(2\alpha s r)\, r dr}{1 - e^{-\alpha R^2}}, \tag{3}$$

where $\alpha = 4\ln 2/\theta_b^2$, R is the disk radius, and I_0 is a zero-order modified Bessel function of the first kind.

In the general case of a beam with i components of FWHM θ_i and peak power amplitude a_i (the integrated power in a given beam is $a_i\theta_i^2 / \sum_i a_i\theta_i^2$) the equation for coupling is:

$$\eta = \frac{\sum_i a_i\theta_i^2\, \eta_i\, w_i}{\sum_i a_i\theta_i^2}. \tag{4}$$

Fitting the measured data with Eq. 4 produces good estimates for the beam FWHMs θ_b, and those can in turn be used to derive the beamwaists from

$$w_o^2 = \frac{1}{2}\left[w^2 \pm \sqrt{w^4 - \left(\frac{2\lambda z}{\pi}\right)^2} \right] \tag{5}$$

where

$$w = \frac{\theta_b}{\sqrt{2\ln 2}}. \tag{6}$$

As a final step, we estimate the edge taper T_e (in dB) for a telescope with f-ratio f/D from the approximate expression

$$T_e = \left(4.63\, w_o \frac{D}{f}\frac{1}{\lambda}\right)^2 . \tag{7}$$

We centered disks with diameters up to 150 mm in the beam at distance $z = 3400$ mm in the laboratory to find that 70% of the power has the distribution that produces a 10.3 dB taper, with the remaining 30% in a very wide angle beam. Figure 3 is a plot of the data and theoretical curves. It is worth noting that it would be hard to find the large scale beam with a small load because η is small in this case; large loads are needed to find the large-scale beams. This is of course a scalar measurement, but the agreement with the design beamwaist size after passage through the optical train is a good sign that the phase fronts are well behaved.

The cryostat, optical, and LO subassemblies are attached to a 0.6 by 0.8 meter commercial optical breadboard table mounted at the right Naysmith focus port of the JCMT. A computer-controlled calibration system with a hot load and ambient chopper for calibrating receiver gain and atmospheric transmission is mounted in the beam just above the receiver. A half-height rack nearby contains bias and control electronics and an IF receiver for tuning.

2.3 Local Oscillator, Intermediate Frequency, and Backend Systems

The local oscillator itself is from Radiometer Physics in Meckenheim, and consists of a 115 GHz Gunn diode oscillator that drives a doubler and then tripler. The oscillator tunes from 659 to 695 GHz with tens of microwatts of power. The phase lock is a STS-800 module connected with a Pacific Millimeter Products model WM 115 GHz harmonic mixer and a HP-8671B frequency synthesizer that provides both the microwave signal for the harmonic mixer and a 100 MHz reference signal for the phase lock loop. A rotatable grid between the LO and diplexer is a variable attenuator for the mixer power level. Typical attenuation levels are around 10 dB. A more elegant solution would have been to vary the bias voltage on the tripler to change the LO chain's output power level electrically.

The IF signal is brought off the mixer contact pads with an unbalanced circuit: one side of the "V" is connected to the mixer block and the other is connected to a $\lambda/4$ IF

transformer. This is a historical holdover, and a balanced IF connection would certainly be better here [11]. Although the dimension of the antenna is small compared with an IF wavelength, the unbalanced connection makes the impedance match somewhat indeterminate by allowing currents to flow to the outside of the mixer block. This is analogous to attempting to make a short circuit by connecting the center conductor of a coax cable to the shield with a wire. No matter how short the wire, the open end of the cable allows currents to be excited on the electrically long outside of the shield. This allows changes far from the end to influence the current distribution, preventing the circuit from being an unambiguous good short.

A short length of coaxial cable brings the signal to a Berkshire Technology 40 dB HEMT amplifier on the helium cold plate. Berkshire provided an integral bias tee for the mixer in the amplifier. We do not use an isolator because it would limit the bandwidth, so the IF matching network in the mixer is the only component that sets the source impedance for the HEMT amplifier. The next amplifier is a low noise Miteq room temperature module with 37 dB gain on the outside of the dewar. A subsequent mix to 4.6 GHz permits us to use a 4–8 GHz IF receiver for tuning, minimizes RFI from other signals at the observatory, and separates the overall system gain in frequency. The signal is sent down a 50–foot long coaxial cable to another IF converter, which converts the band center to 2.2 GHz for the backend spectrometer. All IF components are on thick aluminium plates that are weakly thermally coupled to the external environment for temperature stabilization. The spectrometer is a University of Cologne 1.2 GHz–wide acousto-optical spectrometer with 1.6 MHz noise bandwidth per channel. We enclosed it in a case whose temperature is stabilized by circulated heated water for operation in the observatory dome.

3 Performance at the Telescope

3.1 Internal Measurements

The lower pair of curves on Figure 4 are plots of the mixer junction DC current vs. DC bias voltage with and without the optimum level of local oscillator power. The Josephson currents have been suppressed with a magnetic field, and the lack of structure shows clearly

that the photon energies are slightly larger than the gap energy. The upper pair of curves are the IF power vs. DC bias voltage for ambient and liquid nitrogen temperature black body loads. These curves are smooth and free of fine scale peaks that might indicate magnetic field effects.

The m-shaped curve at the top of Fig. 4 is the IF signal-to-noise ratio: the AC-detected signal divided by the averaged DC signal by an analog ratioing circuit in an Ithaco 391A lock-in amplifier. This curve is reasonably flat away from the Shapiro steps, showing that the exact DC bias voltage point is not very critical. The analog ratioing, the insensitivity to exact bias, and an abundance of LO power allows us to rapidly tune the receiver to optimum.

The noise temperature across the tuning band is shown in Figure 5. The curve is smooth and reproducible; these particular data are typical results from careful but not exceptional tunings made on the last night at the telescope. The noise temperature is about 800 K (DSB) at band center (25 $h\nu/k$), rolling smoothly up to both higher and lower frequencies but remaining below 1000 K over almost the entire 660–690 GHz band.

We made all of these measurements with a liquid nitrogen cold load of diameter 70 mm located 500 mm beyond the diplexer's nominally 6 mm beamwaist. We measured the ambient temperature (5° C) and corrected the liquid nitrogen temperature to 73 K because of the high altitude (the pressure at the telescope is about 0.6 that at sea level). The noise temperature is averaged over the central 500 MHz of the passband, band-limited and measured with a carefully linearized detector system in the 4–8 GHz tuning receiver.

Figure 6 shows the variation of noise temperature across the 1 GHz wide IF band, in this case measured with the acousto-optical spectrometer and the 80° C hot load in the computer-controlled calibration system used during observations. The noise increase at the ends of the superposed astronomical spectrum's baseline (light lines) shows that the effect of the noise rollup near the band edges is acceptable.

Following custom, these receiver temperatures are Rayleigh-Jeans limit temperatures and do not include higher terms. A second order expansion of the Planck equation gives a modified version of the standard Y-factor equation,

$$T_{rec} = \frac{T_H - Y\,T_C}{Y - 1} + \frac{h\nu}{2k}, \tag{8}$$

where T_H, T_C, and Y have their usual meanings of the physical temperatures of the hot and cold loads and the power detector's voltage ratio $Y = V(T_H)/V(T_C)$ for the two loads. At 690 GHz, $h\nu/2k$ = 16.6 K, which is not a large correction.

Although it is difficult to be quantitative at present, the main limit on noise temperature for the present design seems to be some kind of instability noise. The receiver is certainly stable at the gross level, judging from total power strip-chart records and the system Allen variance time of about 30 sec, but this is shorter than the Schottky system's 100 sec and there are occasional steps in total power for no obvious reason. Some low-level instability may come from some interaction between the two not-quite-identical mixers in the array or a lack of simultaneous cancellation of Josephson effects in the two junctions. The IF noise power does depend on the magnetic field strength, but there is a large range of field that has a relatively weak effect on the IF S/N ratio measured with the ratioing circuit. It is also possible that the source impedance presented by the mixer and matching circuit is unfavorable for the first IF amplifier's stability.

Physical temperature effects on noise temperature are weak. Although the gap voltage increased slightly, the sub-gap current decreased, and the corner sharpened somewhat, the 690 GHz noise temperature changed by only 10–15% when the liquid helium bath temperature was reduced from 4.2 K to 1.6 K. The improvement was somewhat larger for the poorer junctions in the sample, but never brought them to the performance of the best junctions.

3.2 Characterizations with Astronomical Measurements

Spectral line observations of astronomical sources are the cleanest test of the overall system. We observed sources we had previously observed with the Schottky system to cross-check the intensity scales, and found agreement within 10%. This agreement in relative calibration shows that the system is either very well behaved or so fiendishly pathological that it imitated normal behavior on our test sources. For one, the agreement showed that "bolometric" effects are completely absent, as one would expect from the smooth IF power vs. DC bias curve. For another, the receiver must be double balanced at at least the 691.5 GHz line frequency. This was theoretically expected from the mixer tuning structure design and

is also suggested experimentally from the smooth tuning curve. Figure 7 shows a more direct measurement, the CO J=6–5 line from Orion observed with the LO both and below the line. The excellent agreement in intensities (no baseline corrections have been made) with a calibration scheme that assumes equal sideband gains is a nearly positive indication that the receiver is very closely double sideband.

The beam distribution is somewhat better than the Schottky system's, and is still heavily influenced by telescope surface errors. We derived the beam distribution on the sky by observing Jupiter (which is a uniform temperature disk to good approximation) at a number of angular offset to vary its coupling to the beam, and then fitting the data to Eq. 4. Figure 8 is a plot of the measured data with the theoretical curve derived from Eqs. 3 and 4. This shows that 40% of the power in the 8″ FWHM "diffraction" beam and the remaining 60% is in a 25″ beam produced by mid-scale antenna surface errors.

4 Conclusion

There is no better conclusion for a paper about a radio astronomical radiometer than to present astronomical data, and Fig. 9 is just that: a map of the Orion outflow made during part of a night of moderate weather. The dramatically increased sensitivity with *FANATIC* made the March 1994 observing run one of the most astronomically fruitful runs we have had. There are obviously several avenues of improvement possible for *FANATIC*. Chief among these are improving the optical coupling. The V-antenna was certainly a good choice historically, but fabrication techniques at these frequencies are also maturing fast, and retrieving the efficiency and background factors of 0.8 in the optics and 0.7 in the beam distribution would drop the present receiver temperature from 800 K to 350 K. Further improvements in AR coating the cold transmission optics and IF matching would drop the receiver temperature well below 10 $h\nu/k$. Now that the noise temperatures are dropping rapidly, and given the possibility of arraying mixers that need only little LO power, high frequency ground-based submillimeter line astronomy will certainly develop rapidly in the next few years.

5 ACKNOWLEDGEMENTS

We thank M. Carter and J. Lamb for their help with the AR coating on the dewar vacuum window, and are very grateful to U. Graf and the University of Cologne mechanical shop for fabricating the large off-axis mirrors. L.J. Tacconi and L. Avery worked very hard in preparations and at the telescope to make the March run a success. The assistance from P. Friberg and the JCMT day crews and staff was, as always, outstanding. This project would not have been possible without the support and encouragement of R. Genzel.

6 REFERENCES

[1] K.-F. Schuster, A.I. Harris, and K.-H. Gundlach 1993, "An SIS Receiver at 690 GHz," *Internat. J. IR and mm Waves* **15**, 1867

[2] J. Zmuidzinas, H.G. LeDuc, J.A. Stern, and S.R. Cypher 1994, "Two-junction Tuning Circuits for Submillimeter SIS Mixers," *IEEE Trans. Microwave Theory Tech.* **42**, no. 4

[3] J.W. Kooi, C.K. Walker, H.G. LeDuc, P.L. Schaffer, T.R. Hunter, D.J. Benford, and T.J. Phillips 1994 "A Low Noise 665 GHz SIS Quasi-Particle Waveguide Receiver," *Internat. J. IR and mm Waves* **15**, 477

[4] M. Salez, P. Febvre, W.R. McGrath, B. Bumble, and H.G. LeDuc 1994, "An SIS Waveguide Heterodyne Receiver for 660-635 GHz, *Internat. J. IR and mm Waves* **15**, 349

[5] J. Mees, S. Crewell, H. Nett, G. de Lange, H. van de Stadt, J.J. Kuipers, R.A. Panhuyzen, "An Airborne SIS Receiver for Atmospheric Measurements at 630 to 720 GHz," these *Proceedings*

[6] A.I. Harris, D.T. Jaffe, J. Stutzki, and R. Genzel 1987, "The UCB/MPE Submillimeter Heterodyne Spectrometer," *Internat. J. IR and mm Waves* **8**, 857

[7] K.-F. Schuster 1993, "Submillimeterspektroskopie in der Umgebung junger Sterne und Entwicklung eines 690 GHz SIS-Empfängers," Ph.D. Thesis, Ludwig-Maximilians-Universität München

[8] A. Eckart, A.I. Harris, and R. Wohlleben 1988, "Scaled Model Measurements of the Sandwiched V-Antenna," *Internat. J. IR and mm Waves* **9**, 505

[9] A.R. Kerr and S.-K. Pan 1990, "Some Recent Developments in the Design of SIS Mixers," *Internat. J. IR and mm Waves* **11**, 1169

[10] J.A. Murphy 1987, "Distortion of a Simple Gaussian Beam on Reflection from Off-Axis Ellipsoidal Mirrors," *Internat. J. IR and mm Waves* **8**, 1165

[11] A.I. Harris, K.-F. Schuster, and L.J. Tacconi 1993, "Broadband IF Matching for Quasioptical Mixers," *Internat. J. IR and mm Waves* **14**, 715

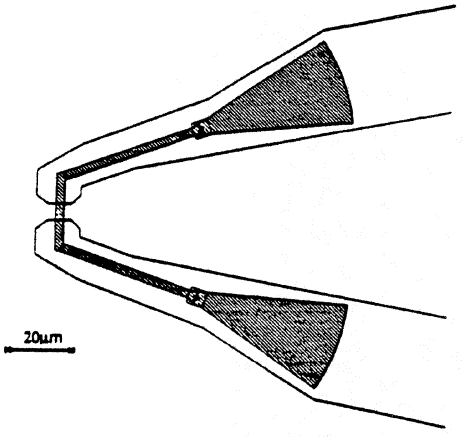

Figure 1: Footpoint of the V-Antenna showing the junctions (small squares), resonators, and transformers. From [1].

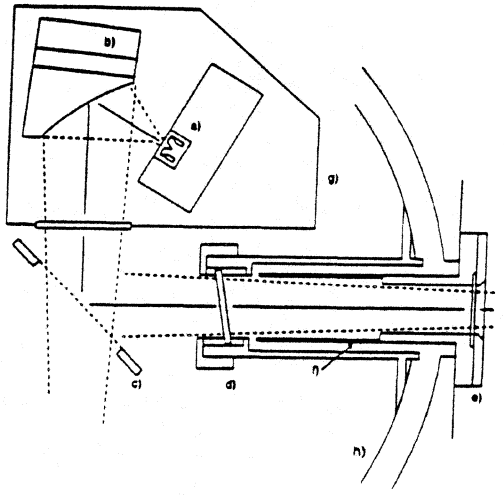

Figure 2: Cryostat internal layout, from [1]. *a*: Mixer; *b*: Off-axis Ellipse; *c*: Wire grid; *d*: Quartz IR filter at 77 K; *e*: AR-coated vacuum window; *f*: RFI suppression tube; *g*: Copper thermal radiation shield housing; *h*: 77 K shield.

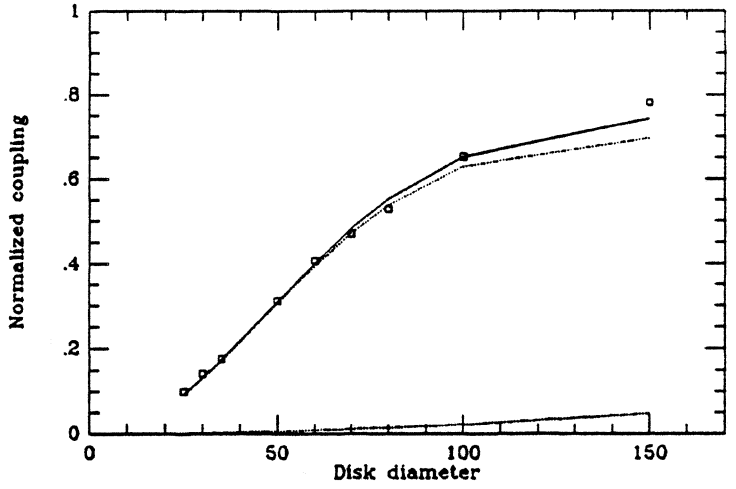

Figure 3: Coupling efficiency of receiver beam to disks of various sizes at z = 3400 mm (crosses), with best-fit theoretical coupling curve (solid lines; Eq. 4). The dotted lines are the individual components, showing the importance of measuring large-scale beams with large loads. 70% of the power is in the smaller beam that couples well to the telescope.

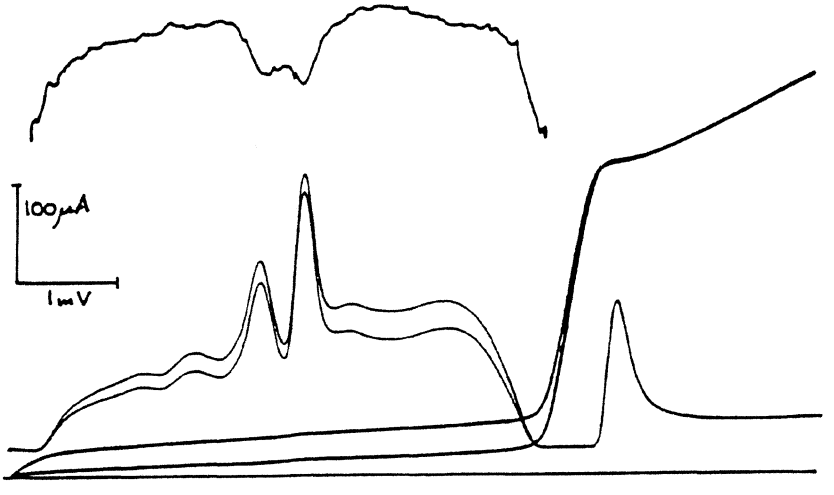

Figure 4: Conversion curves at 690 GHz. The m-shaped curve at the top is the IF signal-to-noise ratio vs. DC bias voltage.

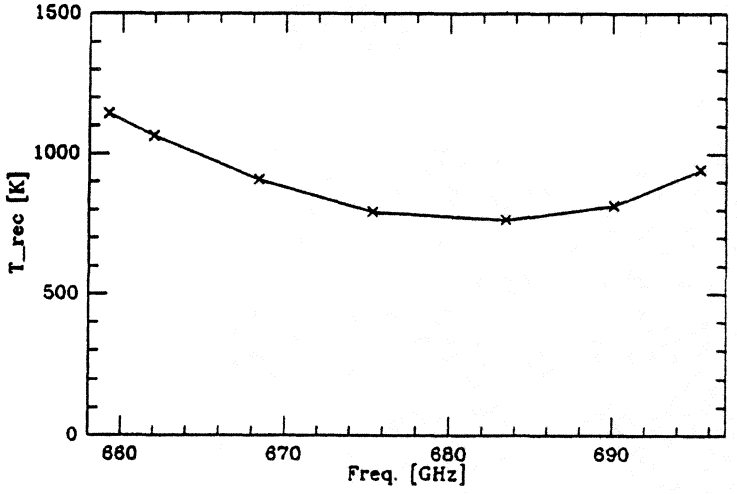

Figure 5: DSB receiver noise temperature vs. tuning frequency, averaged over a 500 MHz IF bandwidth.

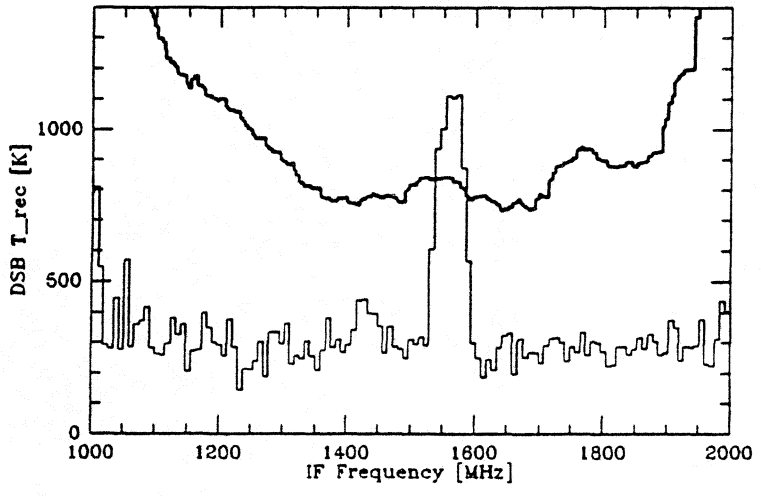

Figure 6: DSB receiver noise temperature vs. IF frequency (heavy lines). The light line spectrum of IRC+10216 shows the effect of increasing noise temperature on the spectral baselines. The baseline is DC shifted to fit in this plot but no tilts or structures have been removed.

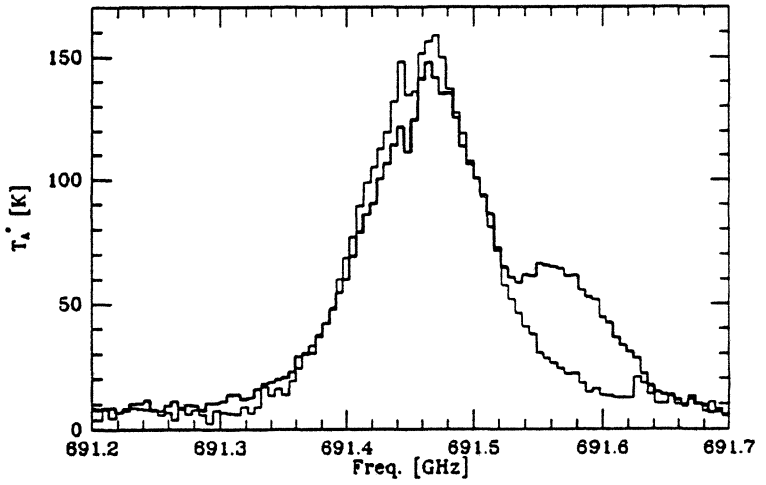

Figure 7: Spectra of the CO J=6–5 line from Orion in both sidebands. The heavy line is USB (and shows a strong line from the other sideband on its wing); the light line is LSB. No baseline corrections have been made, and there is a slight frequency shift due to Orion's 9 km/s LSR velocity. The agreement in peak intensity is within 10% and shows that the receiver is closely double-sideband.

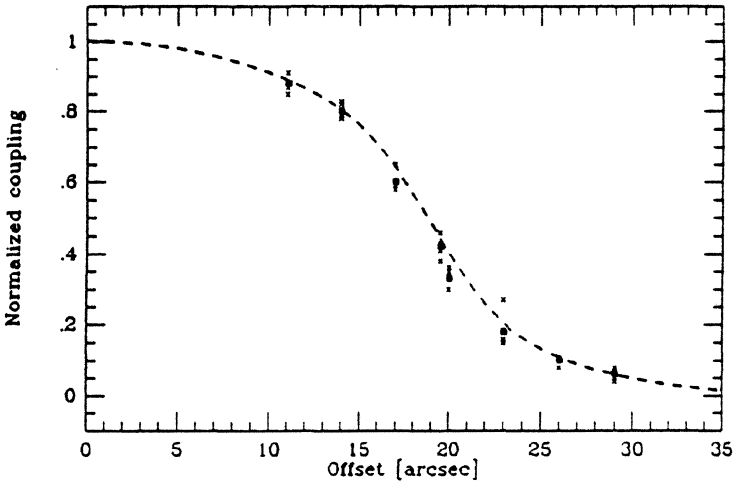

Figure 8: Coupling efficiency of telescope beam to Jupiter for different angular offsets, with best-fit theoretical coupling curve (dashed lines; Eq. 4). Crosses are individual measurements, boxes are the averages. 40% of the power in the 8″ FWHM "diffraction" beam and the remaining 60% is in a 25″ beam produced by mid-scale antenna surface errors.

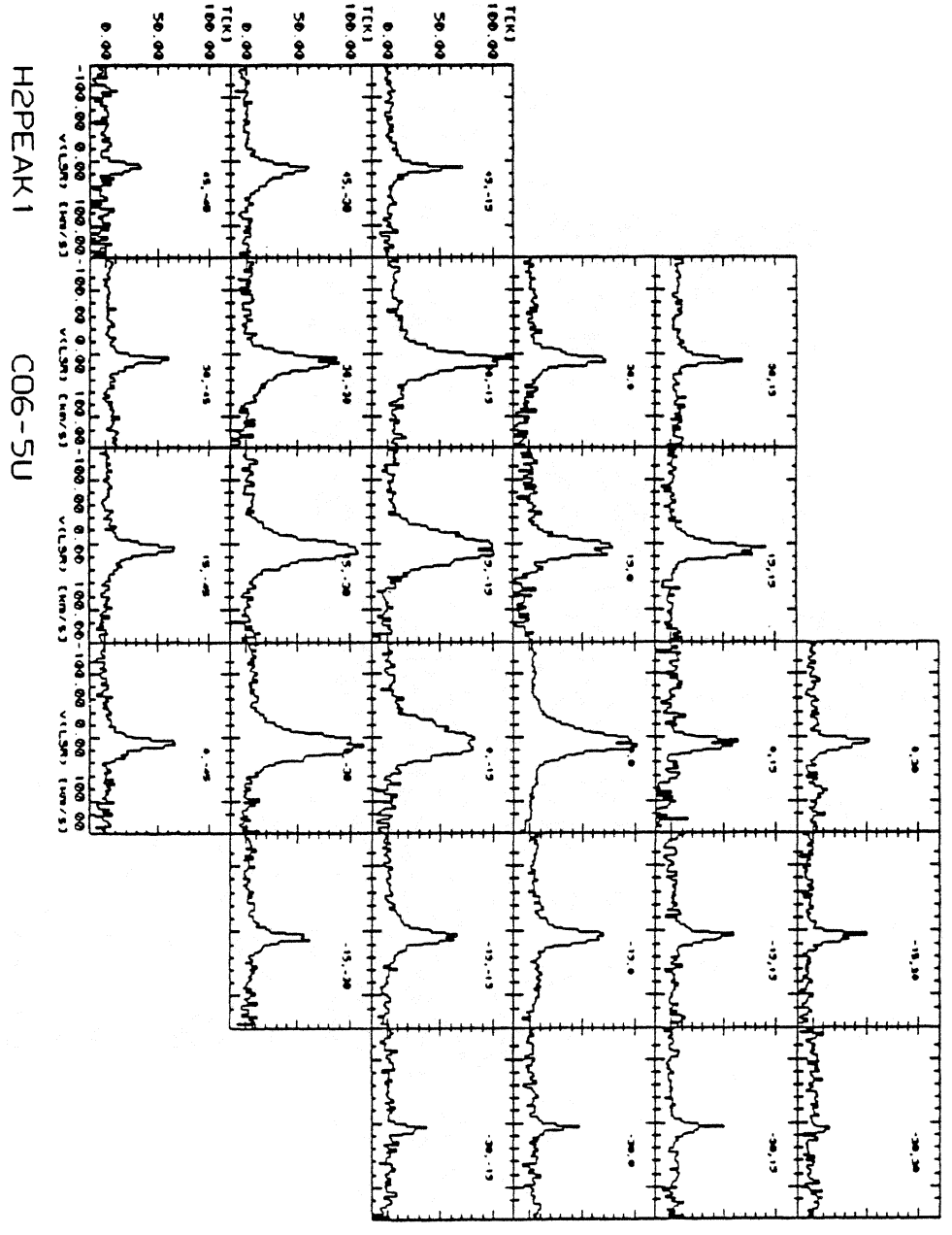

Figure 9: Map of the 691.5 GHz CO J=6-5 map in the Orion outflow. Integration time was 2 min. per point, and no baseline corrections have been made.